Published in final edited form as:
Biomacromolecules. 2009 December 14; 10(12): 3207–3214. doi:10.1021/bm900683r.

Cationic Poly(amidoamine) Dendrimer Induces Lysosomal Apoptotic Pathway at Therapeutically Relevant Concentrations

Thommey P. Thomas[*,†], **Istvan Majoros**[†], **Alina Kotlyar**[†], **Douglas Mullen**[†,‡], **Mark M. Banaszak Holl**[†,‡], and **James R. Baker Jr.**[*,†]

[†] Department of Internal Medicine, Division of Allergy, Michigan Nanotechnology Institute for Medicine and Biological Sciences, University of Michigan, 9220 MSRB III, Box 0648, Ann Arbor, Michigan 48109

[‡] Department of Chemistry, University of Michigan, 930 North University Avenue, Ann Arbor, Michigan 48109

Abstract

Poly(amidoamine) (PAMAM) dendrimers carrying different amounts of surface amino groups were synthesized and tested for their effects on cellular cytotoxicity, lysosomal pH, and mitochondria-dependent apoptosis. In KB cells, the PAMAM dendrimers were taken up into the lysosomal compartment, and they increased the lysosomal pH and cytotoxicity as a function of the number of surface amino groups on the dendrimer. PAMAM dendrimers that were surface-neutralized by acetylation of >80% of the surface amino groups failed to show any cytotoxicity. The positively charged, amine-terminated PAMAM dendrimer induced cellular apoptosis, as demonstrated by mitochondrial membrane potential changes and caspase activity measurements. These results suggest that PAMAM dendrimers are endocytosed into the KB cells through a lysosomal pathway, leading to lysosomal alkalinization and induction of mitochondria-mediated apoptosis.

Introduction

Several polymeric and lipid vectors have recently been developed as alternatives to viral gene delivery systems to overcome the in vivo limitations of the latter, such as immunogenicity, oncogenicity, and toxicity.[1–3] We and others have shown the potential of poly(amidoamine) (PAMAM) dendrimer as a polycationic vector for gene delivery.[4–6] One potential drawback of the use of macromolecular polycationic vectors is their dose-dependent cytotoxicity and decreased transfection efficiency when used below the cytotoxic threshold levels.[7,8] In contrast, low-molecular-weight cationic molecules do not have the toxicity of the macromolecules but are very inefficient gene transfer agents.[9] We have also developed PAMAM dendrimers for use as targeted drug delivery agents for chemotherapeutic applications.[10,11] In those studies, it was found to be crucial to avoid cationic materials in order to obtain selectivity based upon folic acid targeting for both in vitro and in vivo experiments. In practice, this meant carefully neutralizing the amine groups present on the parent dendrimer by exhaustive acylation. Thus, for both gene delivery and targeted chemotherapeutic delivery, the mechanism of polycationic polymer cell uptake and toxicity is of great importance for optimal design of the therapeutic.

The precise mechanisms leading to polycation-induced cytotoxicity are unclear. It is known that the positively charged moieties on a nanosized polymer can interact in concert with

* To whom correspondence should be addressed. thommey@umich.edu (T.P.T.); jbakerjr@umich.edu (J.R.B.).

negatively charged membrane phospholipids.[12,13] Polycationic polymers, including PAMAM dendrimers, poly(ethyleneimine) (PEI), and diethylaminodextran, have been shown to induce the formation of nanoscale holes in model lipid membranes and cause lactate dehydrogenase (LDH) and dye leakage in cell culture experiments at concentrations >200 nM.[12–16] As the polycation-induced plasma membrane porosity is known to be reversible following the removal of the polycationic polymer,[15] it is possible that the mechanisms leading to cell death are also caused by subcellular apoptotic events independent of the transient leakage of cellular materials. A variety of studies have demonstrated that cationic polymers can buffer endolysosomal acidity, the "proton sponge" effect,[17] and it has been proposed that, due to lysosomal swelling and rupture,[18–20] this is important for allowing the efficient delivery and expression of genes using the "polyplexes" of these particles. In contrast, other cationic polyplexes, such as the poly-L-lysine, fail to elicit the proton sponge effect,[21,22] and detailed studies failed to demonstrate a correlation between transfection efficiency and buffering capacity.[23] This raises the question: Could the lysosomal buffering have other important biological effects?

Recent studies have demonstrated a lysosomal pathway for cellular apoptosis.[24–26] Several lysosomotropic agents, such as sphingosine and detergents, are known to trigger lysosomal apoptotic pathways.[27–34] Lysosomal rupture and the release of lysosomal hydrolytic enzymes caused by low doses of the lysosomotropic agents or other external stresses can lead to mitochondrial outer membrane permeabilization (MOMP) and apoptosis, whereas high doses of the same agents may cause cell death through necrosis.[24–27,30,34,35] The observation that protein sponge molecules such as PEI colocalize with lysosomal cathepsin[36] supports a role for lysosomal apoptotic pathway activation in polycation-induced cell death. Given these observations, we designed a set of studies to test the following hypotheses: (1) PAMAM dendrimer-induced cell death occurs via a lysosomal apoptotic pathway, (2) PAMAM dendrimer-induced cell death occurs via cytosolic leakage from the plasma membrane.

To test these hypotheses, the dendrimer-induced cell death pathway was explored using KB cells and Generation 5 PAMAM dendrimers containing varying amounts of primary amines. In a recent report, Generation 4 PAMAM dendrimers at 100–1000 μM (equivalent to 6–60 mM free surface primary amino groups) have been shown to elicit cytotoxicity that was prevented by surface acetylation.[37] In the current study, concentrations up to 3 μM (equivalent to 0.34 mM free surface primary amino groups) were explored, as this is the concentration range that is relevant for therapeutic application, based on previous xenograft mouse studies for chemotherapeutics ($\leq$3 μM) and transfection studies ($\leq$1 μM).[6,10] In addition, unlike the previous reports that employed buffered salt solutions,[15,16,37] the current study used serum-containing cell culture medium for all the incubations with the dendrimers to better simulate the in vivo conditions. The KB cell line was used because this line has been extensively employed as a test cell line for chemotherapeutic applications.[10,11] These studies indicate that PAMAM dendrimers are taken up into the lysosomal compartment and cause an increase in lysosomal pH and cytotoxicity as a function of the number of surface primary amine groups on the dendrimer. In addition, cationic dendrimer-induced cell death involves cellular apoptosis through the lysosomal/mitochondrial pathways.

Experimental Section

Materials

The G5-PAMAM dendrimer (G5-NH_2) was prepared at the Michigan Nanotechnology Institute for Medicine and Biological Sciences, University of Michigan, under GMP-compatible conditions. The Millipore Centricon ultrafiltration membrane YM-10 and the Spectra/Por dialysis membrane (MWCO 10000) were from Fisher. The G5-NH_2 used for conjugation with Alexa Fluor 488 (AF) was purchased from Dendritech Inc. (Midland, MI).

The trypsin-ethylene diamine tetraacetic acid (Trypsin-EDTA), Dulbecco's phosphate-buffered saline (PBS), Hank's balanced salt solution (HBSS), and RPMI 1640 medium were obtained from Gibco/BRL (Gaithersburg, MD). The CytoTox-ONE LDH assay kit was from Promega (Madison, WI), the Mitocapture assay kit was from MBL International (Woburn, MA), and the CaspaTag assay kit was from Chemicon (Temecula, CA). The LysoTracker Red and Alexa Fluor 488 were from Molecular Probes (Eugene, OR). All other reagents were obtained from Sigma-Aldrich (St. Louis, MO) and were used per the manufacturer's protocol. The KB, a subline of the cervical carcinoma HeLa cells (ATCC, Manassas, VA), was grown as a monolayer cell culture at 37 °C and 5% CO_2 in folic acid-deficient RPMI 1640 medium supplemented with 10% fetal bovine serum (FBS). The 10% FBS provided folic acid concentration equivalent to that is present in the human serum (~20 nM).

Synthesis and Characterization of PAMAM Dendrimer with Different Amounts of Surface Primary Amines

Prior to synthesis, the fully amine-terminated G5-NH_2 was analyzed and characterized by ^1H and ^{13}C nuclear magnetic resonance (NMR), matrix-assisted laser desorption ionization time-of-flight (MALDI-TOF), mass spectrometry (MS), high-performance liquid chromatography (HPLC), gel-permeation chromatography (GPC), and polyacrylamide gel electrophoresis as we have described previously.[38] The molecular weight of the G5-NH_2 dendrimer as determined by GPC was 26830 g/mol, and the average number of primary amino groups determined by potentiometric titration was 112.

For the acetylation reaction, the ratio between the acetic anhydride and the dendrimer was adjusted to achieve the acetylation of 20, 40, 60, 80, and 100% (all 112) of the primary amine groups. For the substitution of 20–80% amino groups, weighed aliquots of the dendrimer dissolved in anhydrous methanol were reacted with 1:1 stoichiometric molar amounts of acetic anhydride calculated for the desired amino groups, and complete (100%) acetylation was performed with a 20 mol % excess of the reagent. For example, to obtain 20% acetylation, 1.634×10^{-6} mols of G5-NH_2 was allowed to react with 3.6144×10^{-5} mols of acetic anhydride. Triethylamine, at 20% excess of acetic anhydride, was included in the reaction mixture to quench the acetic acid formed during the reaction. Following 24 h of incubation at room temperature, the mixture was dialyzed in succession in phosphate buffer, pH 7.4, and deionized water, then was lyophilized, and stored at −20 °C. Starting with reaction mixtures containing 43.34, 37.93, 42.00, 40.46, and 41.57 mg each of G5-NH_2, the percent yields of the acetylated dendrimers were 86.5, 82.1, 76.6, 91.3, and 84.6, respectively, for 20, 40, 60, 80, and 100% acetylated products. The molecular weight and the number of amino groups of the synthesized conjugates were determined by GPC, NMR, and MS.

Synthesis of G5-NH_2-Alexa Fluor (G5-NH_2-AF)

To 0.915 μmole of G5-NH_2 dendrimer, dissolved in 5.8 mL phosphate buffered saline (PBS), was added dropwise 1.5 mL of a dimethyl sulfoxide (DMSO) solution of 4.6 μmole of Alexa Fluor 488. The resulting mixture was stirred for 4 days at room temperature under nitrogen, and the product was then purified by size exclusion chromatography using a Sephadex G-25 column and PBS as the eluant. The dendrimer fraction was further purified by ultrafiltration using 10000 MWCO filters (Amicon) and using water as the eluant and was lyophilized. The ^1H NMR integration showed an average of 2.6 Alexa Fluor molecules per dendrimer. HPLC analysis confirmed the removal of all unreacted dye molecules.

Measurement of Lysosomal pH

The lysosomal pH was determined by flow cytometry using a ratiometric analysis of the endolysosomal accumulation of the pH indicator Dextran–Fluorescein conjugate.[39] The cells were cultured on 24-well plates that were incubated with fluorescein isothiocyanate (FITC)-

dextran (0.1 mg/mL final) for 2 days at 37 °C, rinsed, incubated with medium for 3 h to remove excess FITC-dextran attached to the cell surface, and rinsed with medium. The cells were incubated with dendrimers, the medium was removed, they were rinsed with HBSS and trypsinized, and the cell suspensions were prepared. The FL1 (530 ± 28 nm) and FL3 (610 ± 20 nm) fluorescence was measured for the whole cell population using a Beckman-Coulter EPICS-XL MCL flow cytometer, and the data were analyzed using Expo32 software (Beckman-Coulter, Miami, FL). Standard curves were generated using control cells incubated for 10 min with "Britton-Robinson buffers" of pH ranging from 4.5 to 6 and containing sodium azide (10 mM), 2-deoxyglucose (10 mM), and nigericin (10 μM), as described.[39]

Confocal Microscopic Analysis

Cells were seeded at a density of 5×10^5 cells/plate on glass-bottomed culture dishes (Mattek, Ashland, MA) two days prior to the experiment. Cells were incubated with G5-NH_2-AF in cell culture medium under the specified conditions. During the final 1 h of the incubations, the lysosomal dye LysoTracker Red was included, the cells were fixed with paraformaldehyde, and mounted using solution containing the nuclei stain 4,6′-diamidino-2-phenylindole (DAPI). Fluorescent signals were sequentially scanned on an Olympus Fluoview 500 confocal system with an Olympus IX-71 microscope and a 60X water objective to maximize signal separation. DAPI, Alexa Fluor 488 and LysoTracker Red dyes were excited with a 405 nm diode, 488 nm blue argon, and 543 nm HeNe green lasers, respectively. Signals were measured sequentially through 430–460, 505–525, and 560 nm long pass filters. Prior to taking the confocal images, cells were not exposed to the wavelengths from the mercury light source, which can convert the LysoTracker Red to green fluorescent products.[40] Images were magnified 2.5 times with FluoView version 5 software. The *z*-series were taken through representative samples at steps of 0.225 μm with Kalman averaging of two frames. Velocity Software (Improvision Inc., Waltham, MA) was used to quantify the colocalization of G5-NH_2-AF and LysoTracker Red, acquired by averaging the *z*-series images of 10 cells.

XTT Assay

For the cytotoxicity experiments, the cells were seeded in 96-well microtiter plates (3000 cells/well) in serum-containing medium. Two days after plating, the cells were treated with the dendrimers in tissue culture medium under the indicated conditions. A colorimetric "XTT" (sodium 3-[1-(phenylaminocarbonyl)-3,4-tetrazolium]-bis (4-methoxy-6-nitro) benzene sulfonicacid hydrate) assay (Roche Molecular Biochemicals, Indianapolis, IN) was performed following the vendor's protocol. After incubation with the XTT labeling mixture, the microtiter plates were read on an ELISA reader (Synergy HT, BioTek) at 492 nm with the reference wavelength at 690 nm.

LDH Assay

The CytoTox-ONE LDH release assay was conducted as per the manufacture's protocol. The cells cultured in the 96-well plates were treated with dendrimer, followed by incubation for 10 min with a reagent containing a mixture of lactate, nicotinamide adenine dinulceotide (NAD), diaphorase, and a fluorescent precursor substrate resazurin. The fluorescence generated was measured on an ELISA reader (Synergy HT, BioTek) using excitation and emission wavelengths of 560 and 590 nm, respectively. The assay is based on the conversion of lactate to pyruvate by LDH, and the NADH generated in this step is quantitatively utilized for the subsequent conversion by the diaphorase of the substrate resazurin to the fluorescent product resorufin.

Mitochondrial Membrane Depolarization Assay

Cells cultured in 24-well plates were treated with dendrimer; cell suspensions were made by trypsinization, and any cells detached during the dendrimer treatment were pooled. The cells suspended in PBS were incubated with MitoCapture reagent and incubated at 37 °C in the tissue culture incubator for 20 min. The incubation buffer was removed by centrifugation, and the fluorescence of the cells was measured at a 490 nm excitation wavelength and at 530 nm (FL1) and 590 nm (FL3) emission wavelengths, using a Beckman-Coulter EPICS-XL MCL flow cytometer. The assay is based on the principle that in nonapoptotic cells the MitoCapture dye enters the mitochondria and fluoresces at 590 nm, whereas in apoptotic cells the dye remains in the cytoplasm and emits fluorescence at 530 nm.

Caspase Activity Measurement

The CaspaTag caspase activity was performed per the manufacturer's protocol. The cells were cultured and treated with the dendrimer, and the suspensions were prepared as given above. The cells were suspended in serum-free medium and incubated with “fluorochrome inhibitor of caspases (FLICA)” reagent for 1 h at 37 °C under 5% CO_2, protecting the tubes from light. The cells were diluted with wash buffer, centrifuged, rinsed, and incubated with 5 μg/mL propidium iodide (PI) for ~10 min. The FL1 (caspase activity) and FL3 (PI uptake) fluorescence were measured as given above. The assay is based on the detection of active cellular caspases 3 and 7 in apoptotic cells binding to the cell-permeable carboxyfluorescein-labeled caspase inhibitor “FAM-DEVD-FMK” in the FLICA reagent, causing an increase in FL1 fluorescence, and on the uptake of PI into membrane-permeabilized cells.

Results and Discussion

To explore the cationic dendrimer-induced cell death pathway, we employed G5-PAMAM dendrimers because we could control the average charge density per particle by varying the degree of acetylation, $G5(NH_2)_{112-x}(Ac)_x$, on a material with an excellent starting polydispersity index of 1.01. We synthesized and characterized PAMAM dendrimer containing different amounts of surface primary groups. The comparison of the intensity of the NMR peak of the $–CH_3$ of the acetyl groups to the sum-of-intensity of all $–CH_2–$ protons can be used to determine the completion of the acetylation reaction. The ratios of the integral values of $–CH_3$ in the acetyl groups and $–CH_2$ groups in the dendrimer, obtained from the NMR analysis (Figure 1), was in close agreement with the expected theoretical values ranging from 20 to 80% acetylation. We have found that the measured ratio is slightly lower than the theoretical ratio in the case of 100% acetylation (Figure 1). The reason for this discrepancy is that acetic acid, formed during the acetylation by the acetic anhydride, will also react with the primary amino groups, and this side reaction with the amines produces acetate salt. Because of the acetate salt formation in a competing reaction, the rate of amide formation is lower than the rate of amine consumption. The addition of triethylamine to the system competes with the acetic acid side reaction through triethylamine acetate salt formation (a designed reaction to eliminate free acetic acid from the system). The complex nature of the reaction explains why the actual degree of acetylation is different from the theoretical one in the case of 100% acetylation. Similar to the data presented in Figure 1, the molecular weights determined by the GPC and MS methods were similar to the theoretical values within analytical error.

A variety of evidence suggests that polycationic nanoparticles, including PAMAM dendrimers, induce the formation of nanoscale holes, leading to net cell plasma membrane porosity.[12–16] However, for G5-PAMAM dendrimers, the nanoscale hole formation initiates over a concentration range of 200–500 nM, as indicated by bulk LDH assays that we have previously shown not to elicit any acute (<4 h) cytotoxicity as determined by XTT assay.[13,15,16] In this study, we investigated the relationship between the extent of cationic surface amine groups on

PAMAM dendrimer and the cellular pathways leading to the dendrimer-induced cytotoxicity. The cytotoxic potential of a 3 μM solution of G5-PAMAM dendrimer molecules carrying different amounts of surface amino groups as determined by the release of cellular LDH is illustrated in Figure 2. Dendrimers containing 40–100% surface amino groups showed a time-dependent release of LDH from KB cells, whereas the fully acetylated dendrimers and dendrimers with only 20% of the initial surface amino groups failed to show any significant LDH leakage after a 2 h incubation. Only modest increases in LDH release were observed with the addition of the 40–80% amine-terminated dendrimers. In contrast, dendrimers with 100% amine surfaces showed a significantly greater cytotoxicity, causing about 82% of the total cellular LDH to be released into the extracellular fluid.

To examine if polycationic dendrimer-induced cell death was the result of the formation of membrane pores[13,16] and a result of dendrimer endocytosis leading to cell death through the lysosomal apoptotic pathways,[22,26,41] we performed the following experiments. First, we examined the intracellular localization of Alexa Fluor-labeled G5-NH_2 (G5-NH_2-AF) dendrimer in the KB cells. In agreement with the lysosomal localization of G2 dendrimer in the colorectal cancer cell line Caco-2,[42] our study shows the rapid accumulation of the G5-NH_2 PAMAM dendrimer in the lysosomal compartment of the KB cells (Figure 3). The discrete punctate appearance of the dendrimer green fluorescence and the colocalization of the dendrimer with the lysosome-specific dye LysoTracker Red suggest that there is significant dendrimer uptake in these cells via the lysosomal pathway. Control cells treated with PBS, imaged under identical conditions, failed to show any green fluorescence (Figure 3E), indicating that the observed green fluorescence is not due to light-induced conversion of the Lysotracker dye to green fluorescent products as has been reported previously.[40] Pixel intensity analysis of the colocalization of a field of 10 cells showed that, in 1 h, 58% of all the green dendrimer fluorescence colocalized with the red LysoTracker fluorescence and 80% of all the red fluorescence colocalized with the green dendrimer fluorescence.

Given the well-documented lysosomal activity of cationic dendrimer particles,[18–20] we then investigated whether the particles could induce a lysosomal pathway to cell death.[27–33] We evaluated the possibility that the accumulation of cationic dendrimer in the lysosomal compartment leads to changes in the lysosomal pH. Polyplexes labeled with pH-sensitive dyes have been previously employed to follow the kinetics of the trafficking of the particles through different cellular compartments having varying pHs.[22,23] In those studies, the lysosomal pH was determined by the fluorescence emission of a pH-sensitive dye labeled onto the surface of an internalized cationic nanoparticle. As those particles may also buffer the lysosomes, determination of an increase in pH cannot be accurately discerned. Those methods although track the spatiotemporal variations in cellular pH during the nanoparticle trafficking, they do not provide the basal pH and the actual changes in pH units of the endolysosomal compartment. In this study, we used Dextran-FI, known to accumulate into lysosomes for accurate assessment of the basal pH as well as any changes in the lysosomal pH.[39] The time- and dose-dependent change in lysosomal pH as a function of exposure to a G5-PAMAM dendrimer solution is illustrated in Figure 4. At 300 nM, a shift of ~0.3 pH units more basic was observed in less than 20 min, and a maximal shift of ~0.5 pH units was observed at 1–3 μM. Note that the lysosomal pH increases faster than the LDH release response. Furthermore, the lysosomes become alkaline at concentrations that we have previously shown not to release substantial LDH.[13,15,16]

The relationship between the degree of amine termination, the increase in lysosomal pH, the LDH release, and the cell cytotoxicity was examined as a function of the number of dendrimer surface amine groups. As illustrated in Figure 5, the lysosomal pH (circle symbols), cell death as determined by either flow cytometry (diamond symbols; obtained from the number of cells in the dead/apoptotic population identified in the forward scatter/side scatter plot), and cell

proliferation as determined by XTT assay (square symbols) exhibit the same overall trend, whereas the LDH response (triangle symbols) is substantially less until the lysis conditions are reached. In Figure 5, the data is represented as the percent maximal changes to show trends in the relative increases for each parameter. The maximum effects caused by 3 μM 100% amine-terminated dendrimer under these conditions were as follows: 0.5 pH unit change in 1 h; ~8% of a total of 10000 cells appearing in the dead/apoptotic population in the side scatter/forward scatter plot of flow cytometry in 1 h; 50 and 82% of the total cellular LDH released, respectively, in 1 and 2 h; and >95% cell growth inhibition in 3 days as determined by the XTT assay.

The data presented in Figures 2 and 5 show that, despite causing only a modest increase in LDH release by dendrimers containing up to ~80% surface primary amines, there is a significant acute increase in the lysosomal pH. In addition, the trends of the increases in cytotoxicity as determined by flow cytometry and by XTT assay, but not of the LDH release, were similar to the increases in the lysosomal pH increase. These results suggest that a minimum level of surface primary amino groups (40–60% at 3 μM) is required as a threshold for acute dendrimer-induced membrane disruption and LDH release. In the flow cytometric analysis (Figure 5), although the maximum cell killing caused by the 100% amine-surfaced dendrimer was only ~8% of the total cells in 1 h, there was a progressive acute increase in the number of apoptotic/dead cells (out of 10000 cells analyzed) caused by 40–80% amine-surfaced dendrimer. This suggests that 40–80% of dendrimer primary amines (equivalent to ~120–240 μM primary amines) can cause significant increases in lysosomal pH, followed by the initiation of acute cell death leading to cell growth inhibition without a proportionate increase in the LDH release. Above this threshold, the dendrimer evoked cytotoxicity as determined by all the different methods employed, including the LDH release. Indeed, by all measures employed, the cytotoxicity was negligible for dendrimers containing 0–20% surface amino groups at $a \leq 3$ μM concentration. This finding is especially significant as a design principle for multifunctional targeted dendrimer nanodevices such as “G5-folic acid-dye-methotrexate”.[10,11,43] The total number of charged groups should be kept under ~20% to minimize the charge-based interactions leading to cytotoxicity and ideally kept to a minimum. The precise cellular mechanism of action of the differentially acetylated dendrimers is not evident from the current study. Our previous confocal microscopy studies have shown that fluorescently labeled and fully acetylated dendrimers fail to endocytose into KB cells.[11] Therefore the differential cellular effects elicited by the 0–100% acetylated dendrimers could be due to the differences in their cellular uptake levels, and the net positive charges delivered into the cell.

The effect of different lysosome-disrupting agents on lysosomal pH and cell growth was compared with the effects elicited by the PAMAM dendrimers (Figure 6). The lysosomotropic agent chloroquine, which is also known to increase the lysosomal pH and disrupt the lysosomal membrane,[44–46] caused a significant increase in the lysosomal pH and the cytotoxicity in the KB cells. Similarly, bafilomycin A1, an inhibitor of vacuolar H^+-ATPase,[47,48] increased both the lysosomal pH and decreased cell viability in the KB cells. Incubation of these cells with G5-NH_2 at 1 μM (Figure 6) or at 3 μM (Figures 4 and 5) resulted in a significant induction of cell death and an increase in lysosomal pH to >5.0, whereas incubation with 100% surface-neutralized G5-NH-Ac dendrimer resulted in no toxicity and no pH change.

The effect of dendrimer exposure upon the mitochondrial transmembrane potential (MTP) was determined by flow cytometric analysis using the MitoCapture assay described in the Experimental Section. The forward scatter/side scatter plots revealed two cell populations, designated as live (*L*) and apoptotic or dead (*A*), based on the extent of light scattering. The G5-NH_2 produced an ~30% increase in the apoptotic population by 2 h after treatment, and 100% of the cells were apoptotic at 24 h after exposure (Figure 7, upper panel). As part of this

analysis, it appeared that the MTP reached a maximum in 2 h (Figure 7, lower panel). In contrast, the positive control staurosporine under similar conditions was less effective at inducing cell death, with insignificant apoptosis at 2 h and only ~18% cell death at 24 h after exposure. Staurosporine-treated cells also required 24 h to achieve a MTP level similar to the maximal level reached by the G5-NH_2 at 2 h. There were no significant changes in the MTP in the remaining live cell populations (population *L*) under all conditions.

As activation of the cysteine-aspartic acid proteases (caspases) plays a critical role in the apoptotic execution, the effect of the PAMAM dendrimer on caspase activity was measured. The CaspaTag assay used in the study determines the activity of caspases 3 and 7, which are two known "effector" caspases involved in the final execution of the apoptotic pathway. Similar to the results shown in Figure 7, dendrimer and staurosporine treatment of the KB cells resulted in the identification of two cell populations (populations *L* and *A*) in the forward scatter/side scatter analysis (data not shown). The amine-terminated dendrimer increased the caspase activity significantly in 2 h, with most activity observed in population *A* (Figure 8, middle panels). The increased caspase activity also coincided with an increase in propidium iodide staining. In 24 h, the PAMAM dendrimer caused all the cells to be in population *A*, which was also all positive to caspase activity and propidium iodide staining (bottom left panel), similar to the known KB cell apoptotic agent staurosporine (right panels).[49]

As originally proposed by Christian de Duve, the discoverer of lysosomes, the mechanism of the pinocytosed cationic PAMAM dendrimer-induced cell death pathway may involve the nonprotonated surface amino groups acting as a proton sponge and causing endolysosomal neutralization, osmotic swelling, membrane rupture, and the exit of lysosomal enzymes, leading to cell death.[50] This is evidenced from the observations that the dendrimer increases lysosomal pH and cytotoxicity as a function of the surface amino groups, they get localized in the lysosomal compartment, and they cause mitochondrial mediated apoptosis that has previously been shown to occur as a consequence of lysosomal breakdown and cathepsin release.[25,27,30,33,51–55] The dose–response curves (Figure 5) showed strong correlations between the number of surface amino groups and increases in lysosomal pH as well as cell death, suggesting a role of the lysosomal alkalinization for the dendrimer-induced cell death. This is further supported by the observation that in the KB cells, the G5-NH_2 dendrimer and the known lysosomotropic agents chloroquine and Bafilomycin A induced both lysosomal-mediated cell death as well as increases in lysosomal pH (Figure 6). Our finding on dendrimer-induced apoptosis raises concerns on the usage of DNA complexes with positively charged polymers (polyplexes) as gene-delivery agents, known to be taken up into cells by endocytosis through the endosomal/lysosomal pathway.[19,56] However, further studies are needed to establish if the apoptotic induction observed for the free dendrimer may be extended to DNA-polyplexes.

Conclusions

PAMAM dendrimer-induced cell death is shown to follow a lysosome-induced pathway to apoptotic cell death for therapeutically relevant concentrations of dendrimer. The nanoscale hole formation that can lead to LDH leakage at these concentrations does not appear to cause early cytotoxicity as previously noted,[13,15,16] and the induction of apoptosis plays the major role in dendrimer-induced cell death. These studies also indicate that neither LDH leakage nor the lysosomal cell death pathway is expected to be active for the targeted chemotherapeutic devices previously reported that employed surface-neutralized dendrimers.[10,11] However, the role of this lysosomal toxicity in the optimization of polycationic polyplexes for gene delivery, and for drug delivery using uncapped positively charged dendrimers, is clearly a substantial concern.

Acknowledgments

This project has been funded in whole or in part with Federal funds from the National Cancer Institute, National Institutes of Health, under Awards 1 R33 CA112141 and 1 R21 RR021893, and the National Institute of Biomedical Imaging and Bio-Engineering, National Institutes of Health, under Award RO1 EB005028. This work utilized the Morphology and Image Analysis Core of the Michigan Diabetes Research and Training Center funded by NIH5P60 DK20572 from the National Institute of Diabetes and Digestive and Kidney Diseases. We thank Dr. Stephen I. Lentz for his skillful technical help in the confocal microscopic analysis. We also thank Douglas Mullen, graduate student, in assisting with the synthesis of Alexa Fluor-conjugated dendrimer. Dr. James R. Baker, Jr. holds an ownership position in Avidimer Therapeutics, Inc. and is the inventor of technologies that the University has licensed to Avidimer Therapeutics, Inc., and some of these technologies are involved in this research. Avidimer Therapeutics, Inc. had no role in the study design, data collection and analysis, decision to publish, or preparation of the manuscript.

References and Notes

1. Agarwal A, Mallapragada SK. Synthetic sustained gene delivery systems. Curre Top Med Chem 2008;8 (4):311–0.
2. de Wolf HK, Luten J, Snel CJ, Storm G, Hennink WE. Biodegradable, cationic methacrylamide-based polymers for gene delivery to ovarian cancer cells in mice. Mol Pharmaceutics 2008;5(2):349–57.
3. Luten J, van Nostrum CF, De Smedt SC, Hennink WE. Biodegradable polymers as non-viral carriers for plasmid DNA delivery. J Controlled Release 2008;126(2):97–110.
4. Baker JR Jr, Bielinska AU, Kukowska-Latallo JF. Dendrimer-mediated cell transfection in vitro. Methods Mol Biol 2004;245:67–82. [PubMed: 14707370]
5. Hui Z, He ZG, Zheng L, Li GY, Shen SR, Li XL. Studies on polyamidoamine dendrimers as efficient gene delivery vector. J Biomater Appl 2008;22(6):527–44. [PubMed: 17623709]
6. Kukowska-Latallo JF, Bielinska AU, Johnson J, Spindler R, Tomalia DA, Baker JR Jr. Efficient transfer of genetic material into mammalian cells using Starburst polyamidoamine dendrimers. Proc Natl Acad Sci USA 1996;93(10):4897–902. [PubMed: 8643500]
7. Douglas KL, Piccirillo CA, Tabrizian M. Cell line-dependent internalization pathways and intracellular trafficking determine transfection efficiency of nanoparticle vectors. Eur J Pharm Biopharm 2008;68 (3):676–87. [PubMed: 17945472]
8. Godbey WT, Wu KK, Mikos AG. Poly(ethylenimine)-mediated gene delivery affects endothelial cell function and viability. Biomaterials 2001;22(5):471–80. [PubMed: 11214758]
9. Kunath K, von Harpe A, Fischer D, Petersen H, Bickel U, Voigt K, Kissel T. Low-molecular-weight polyethylenimine as a non-viral vector for DNA delivery: Comparison of physicochemical properties, transfection efficiency and in vivo distribution with high-molecular-weight polyethylenimine. J Controlled Release 2003;89(1):113–25.
10. Kukowska-Latallo JF, Candido KA, Cao Z, Nigavekar SS, Majoros IJ, Thomas TP, Balogh LP, Khan MK, Baker JR Jr. Nanoparticle targeting of anticancer drug improves therapeutic response in animal model of human epithelial cancer. Cancer Res 2005;65(12):5317–24. [PubMed: 15958579]
11. Thomas TP, Majoros IJ, Kotlyar A, Kukowska-Latallo JF, Bielinska A, Myc A, Baker JR Jr. Targeting and inhibition of cell growth by an engineered dendritic nanodevice. J Med Chem 2005;48(11):3729–35. [PubMed: 15916424]
12. Leroueil PR, Berry SA, Duthie K, Han G, Rotello VM, McNerny DQ, Baker JR Jr, Orr BG, Holl MM. Wide varieties of cationic nanoparticles induce defects in supported lipid bilayers. Nano Lett 2008;8(2):420–4. [PubMed: 18217783]
13. Leroueil PR, Hong S, Mecke A, Baker JR Jr, Orr BG, Banaszak Holl MM. Nanoparticle interaction with biological membranes: Does nanotechnology present a Janus face. Acc Chem Res 2007;40(5): 335–42. [PubMed: 17474708]
14. Fischer D, Li Y, Ahlemeyer B, Krieglstein J, Kissel T. In vitro cytotoxicity testing of polycations: Influence of polymer structure on cell viability and hemolysis. Biomaterials 2003;24(7):1121–31. [PubMed: 12527253]
15. Hong S, Bielinska AU, Mecke A, Keszler B, Beals JL, Shi X, Balogh L, Orr BG, Baker JR Jr, Banaszak Holl MM. Interaction of poly(amidoamine) dendrimers with supported lipid bilayers and cells: Hole formation and the relation to transport. Bioconjugate Chem 2004;15(4):774–82.

16. Hong S, Leroueil PR, Janus EK, Peters JL, Kober MM, Islam MT, Orr BG, Baker JR Jr, Banaszak Holl MM. Interaction of polycationic polymers with supported lipid bilayers and cells: Nanoscale hole formation and enhanced membrane permeability. Bioconjugate Chem 2006;17(3):728–34.
17. Behr JP. Synthetic gene-transfer vectors. Acc Chem Res 1993;26(5):274–278.
18. Akinc A, Thomas M, Klibanov AM, Langer R. Exploring polyethylenimine-mediated DNA transfection and the proton sponge hypothesis. J Gene Med 2005;7(5):657–63. [PubMed: 15543529]
19. Sonawane ND, Szoka FC Jr, Verkman AS. Chloride accumulation and swelling in endosomes enhances DNA transfer by polyamine–DNA polyplexes. J Biol Chem 2003;278(45):44826–31. [PubMed: 12944394]
20. Kichler A, Leborgne C, Coeytaux E, Danos O. Polyethylenimine-mediated gene delivery: A mechanistic study. J Gene Med 2001;3(2):135–44. [PubMed: 11318112]
21. Akinc A, Langer R. Measuring the pH environment of DNA delivered using nonviral vectors: Implications for lysosomal trafficking. Biotechnol Bioeng 2002;78(5):503–8. [PubMed: 12115119]
22. Forrest ML, Pack DW. On the kinetics of polyplex endocytic trafficking: Implications for gene delivery vector design. Mol Ther 2002;6(1):57–66. [PubMed: 12095304]
23. Kulkarni RP, Mishra S, Fraser SE, Davis ME. Single cell kinetics of intracellular, nonviral, nucleic acid delivery vehicle acidification and trafficking. Bioconjugate Chem 2005;16(4):986–94.
24. Brunk UT, Neuzil J, Eaton JW. Lysosomal involvement in apoptosis. Redox Rep 2001;6(2):91–7. [PubMed: 11450988]
25. Guicciardi ME, Leist M, Gores GJ. Lysosomes in cell death. Oncogene 2004;23(16):2881–90. [PubMed: 15077151]
26. Kroemer G, Jaattela M. Lysosomes and autophagy in cell death control. Nature Rev Cancer 2005;5 (11):886–97. [PubMed: 16239905]
27. Boya P, Andreau K, Poncet D, Zamzami N, Perfettini JL, Metivier D, Ojcius DM, Jaattela M, Kroemer G. Lysosomal membrane permeabilization induces cell death in a mitochondrion-dependent fashion. J Exp Med 2003;197(10):1323–34. [PubMed: 12756268]
28. Boya P, Gonzalez-Polo RA, Poncet D, Andreau K, Vieira HLA, Roumier T, Perfettini JL, Kroemer G. Mitochondrial membrane permeabilization is a critical step of lysosome-initiated apoptosis induced by hydroxychloroquine. Oncogene 2003;22(25):3927–36. [PubMed: 12813466]
29. Boya P, Morales MC, Gonzalez-Polo RA, Andreau K, Gourdier I, Perfettini JL, Larochette N, Deniaud A, Baran-Marszak F, Fagard R, Feuillard J, Asumendi A, Raphael M, Pau B, Brenner C, Kroemer G. The chemopreventive agent *N*-(4-hydroxyphenyl)retinamide induces apoptosis through a mitochondrial pathway regulated by proteins from the Bcl-2 family. Oncogene 2003;22(40):6220–30. [PubMed: 13679861]
30. Cirman T, Oresic K, Mazovec GD, Turk V, Reed JC, Myers RM, Salvesen GS, Turk B. Selective disruption of lysosomes in HeLa cells triggers apoptosis mediated by cleavage of Bid by multiple papain-like lysosomal cathepsins. J Biol Chem 2004;279(5):3578–87. [PubMed: 14581476]
31. Droga-Mazovec G, Bojic L, Petelin A, Ivanova S, Romih R, Repnik U, Salvesen GS, Stoka V, Turk V, Turk B. Cysteine cathepsins trigger caspase-dependent cell death through cleavage of bid and antiapoptotic Bcl-2 homologues. J Biol Chem 2008;283(27):19140–50. [PubMed: 18469004]
32. Li W, Yuan XM, Ivanova S, Tracey KJ, Eaton JW, Brunk UT. 3-Aminopropanal, formed during cerebral ischaemia, is a potent lysosomotropic neurotoxin. Biochem J 2003;371(Pt 2):429–36. [PubMed: 12513695]
33. Bidere N, Lorenzo HK, Carmona S, Laforge M, Harper F, Dumont C, Senik A. Cathepsin D triggers Bax activation, resulting in selective apoptosis-inducing factor (AIF) relocation in T lymphocytes entering the early commitment phase to apoptosis. J Biol Chem 2003;278(33):31401–11. [PubMed: 12782632]
34. Kagedal K, Zhao M, Svensson I, Brunk UT. Sphingosine-induced apoptosis is dependent on lysosomal proteases. Biochem J 2001;359(Pt 2):335–43. [PubMed: 11583579]
35. Li N, Zheng Y, Chen W, Wang C, Liu X, He W, Xu H, Cao X. Adaptor protein LAPF recruits phosphorylated p53 to lysosomes and triggers lysosomal destabilization in apoptosis. Cancer Res 2007;67(23):11176–85. [PubMed: 18056442]

36. Lecocq M, Wattiaux-De Coninck S, Laurent N, Wattiaux R, Jadot M. Uptake and intracellular fate of polyethylenimine in vivo. Biochem Biophys Res Commun 2000;278(2):414–8. [PubMed: 11097851]
37. Kolhatkar RB, Kitchens KM, Swaan PW, Ghandehari H. Surface acetylation of polyamidoamine (PAMAM) dendrimers decreases cytotoxicity while maintaining membrane permeability. Bioconjugate Chem 2007;18(6):2054–60.
38. Majoros IJ, Thomas TP, Mehta CB, Baker JR Jr. Poly(amidoamine) dendrimer-based multifunctional engineered nanodevice for cancer therapy. J Med Chem 2005;48(19):5892–9. [PubMed: 16161993]
39. Nilsson C, Kagedal K, Johansson U, Ollinger K. Analysis of cytosolic and lysosomal pH in apoptotic cells by flow cytometry. Methods Cell Sci 2003;25(3–4):185–94. [PubMed: 15801164]
40. Freundt EC, Czapiga M, Lenardo MJ. Photoconversion of Lysotracker Red to a green fluorescent molecule. Cell Res 2007;17(11):956–8. [PubMed: 17893709]
41. Griffiths PC, Paul A, Khayat Z, Wan KW, King SM, Grillo I, Schweins R, Ferruti P, Franchini J, Duncan R, Wan KW. Understanding the mechanism of action of poly(amidoamine)s as endosomolytic polymers: Correlation of physicochemical and biological properties. Biomacromolecules 2004;5(4):1422–7. [PubMed: 15244460]
42. Kitchens KM, Foraker AB, Kolhatkar RB, Swaan PW, Ghandehari H, Kitchens KM, Foraker AB, Kolhatkar RB, Swaan PW, Ghandehari H. Endocytosis and interaction of poly (amidoamine) dendrimers with Caco-2 cells. Pharm Res 2007;24(11):2138–45. [PubMed: 17701324]
43. Thomas, TP.; Shukla, R.; Majoros, IJ.; Myc, A.; Baker, JR, Jr. Poly (amidoamine) dendrimer-based multifunctional nanoparticles. In: Mirkin, editor. Nanobiotechnology: Concepts, Methods and Perspectives. Wiley-VCH; New York: 2007.
44. Mahon GJ, Anderson HR, Gardiner TA, McFarlane S, Archer DB, Stitt AW. Chloroquine causes lysosomal dysfunction in neural retina and RPE: Implications for retinopathy. Curr Eye Res 2004;28 (4):277–84. [PubMed: 15259297]
45. Ji J, Rosenzweig N, Griffin C, Rosenzweig Z. Synthesis and application of submicrometer fluorescence sensing particles for lysosomal pH measurements in murine macrophages. Anal Chem 2000;72(15):3497–503. [PubMed: 10952534]
46. Wattiaux R, Jadot M, Warnier-Pirotte MT, Wattiaux-De Coninck S. Cationic lipids destabilize lysosomal membrane in vitro. FEBS Lett 1997;417(2):199–202. [PubMed: 9395295]
47. Tapper H, Sundler R. Bafilomycin A1 inhibits lysosomal, phagosomal, and plasma membrane H(+)-ATPase and induces lysosomal enzyme secretion in macrophages. J Cell Physiol 1995;163(1):137–44. [PubMed: 7896890]
48. Nakashima S, Hiraku Y, Tada-Oikawa S, Hishita T, Gabazza EC, Tamaki S, Imoto I, Adachi Y, Kawanishi S. Vacuolar H+-ATPase inhibitor induces apoptosis via lysosomal dysfunction in the human gastric cancer cell line MKN-1. J Biochem 2003;134(3):359–64. [PubMed: 14561721]
49. Myc A, Majoros IJ, Thomas TP Jr. Dendrimer-based targeted delivery of an apoptotic sensor in cancer cells. Biomacromolecules 2007;8(1):13–18. [PubMed: 17206782]
50. de Duve C, de Barsy T, Poole B, Trouet A, Tulkens P, Van Hoof F. Commentary. Lysosomotropic agents. Biochem Pharmacol 1974;23(18):2495–531. [PubMed: 4606365]
51. Bivik C, Rosdahl I, Ollinger K. Hsp70 protects against UVB induced apoptosis by preventing release of cathepsins and cytochrome c in human melanocytes. Carcinogenesis 2007;28(3):537–44. [PubMed: 16950797]
52. Chen W, Li N, Chen T, Han Y, Li C, Wang Y, He W, Zhang L, Wan T, Cao X. The lysosome-associated apoptosis-inducing protein containing the pleckstrin homology (PH) and FYVE domains (LAPF), representative of a novel family of PH and FYVE domain-containing proteins, induces caspase-independent apoptosis via the lysosomal-mitochondrial pathway. J Biol Chem 2005;280 (49):40985–95. [PubMed: 16188880]
53. Broker LE, Kruyt FAE, Giaccone G. Cell death independent of caspases: A review. Clin Cancer Res 2005;11(9):3155–62. [PubMed: 15867207]
54. Esteves-Souza A, Lucio KA, Da Cunha AS, Da Cunha Pinto A, Da Silva Lima EL, Camara CA, Vargas MD, Gattass CR. Antitumoral activity of new polyamine-naphthoquinone conjugates. Oncol Rep 2008;20(1):225–31. [PubMed: 18575741]

55. Yang J, Wu LJ, Tashino SI, Onodera S, Ikejima T. Reactive oxygen species and nitric oxide regulate mitochondria-dependent apoptosis and autophagy in evodiamine-treated human cervix carcinoma HeLa cells. Free Radical Res 2008;42(5):492–504. [PubMed: 18484413]

56. Breunig M, Lungwitz U, Liebl R, Fontanari C, Klar J, Kurtz A, Blunk T, Goepferich A. Gene delivery with low molecular weight linear polyethylenimines. J Gene Med 2005;7(10):1287–98. [PubMed: 15906395]

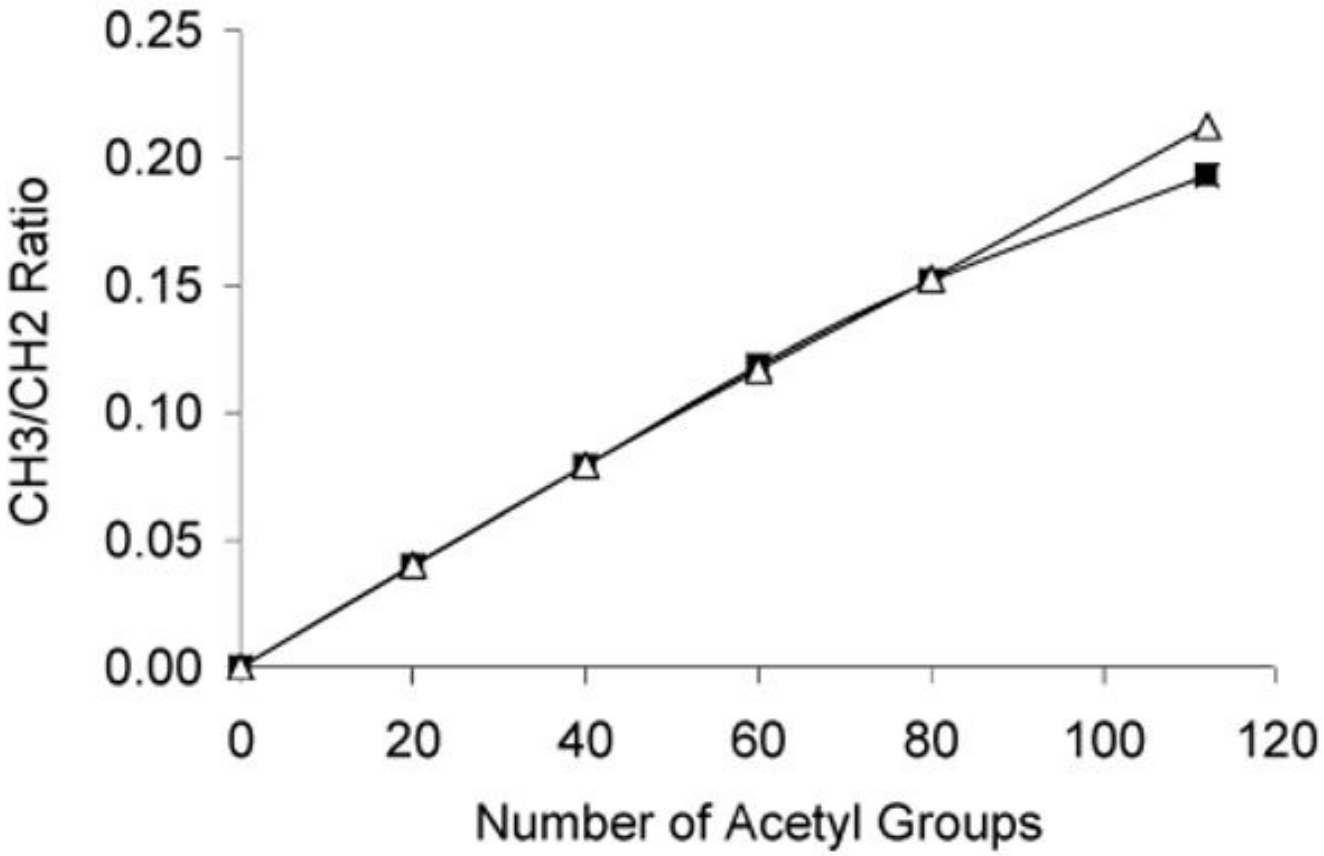

Figure 1.
Comparison of the proton ratio of $–CH_3$ in the acetyl groups and all $–CH_2$ groups in the dendrimer structure vs number of primary amine groups acetylated. The data is given as the ratio of the number of protons in methyl groups generated by acetylation vs the number of protons in methylene groups in the interior of dendrimer. The open symbols show the theoretical values, and the filled symbols show the measured ratio calculated from the NMR data.

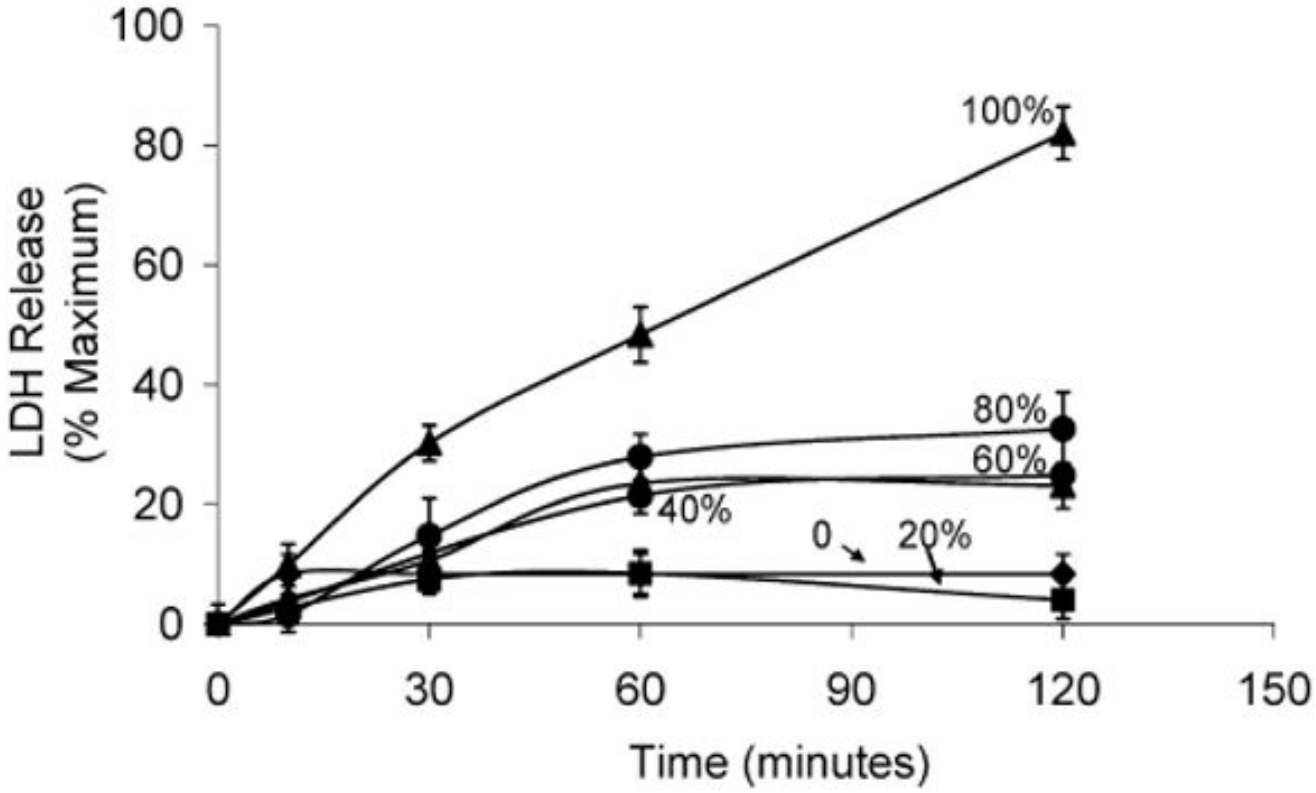

Figure 2.

Time-dependent cytotoxicity of PAMAM dendrimers having varying amounts of primary amine groups. KB cells were incubated at 37 °C with 3 μM each of PAMAM dendrimers carrying 0–100% of surface primary amino groups, and the cytotoxicity was determined by LDH release assay. The data are expressed as the percentages of the maximal LDH release obtained for Triton X-lysed cells.

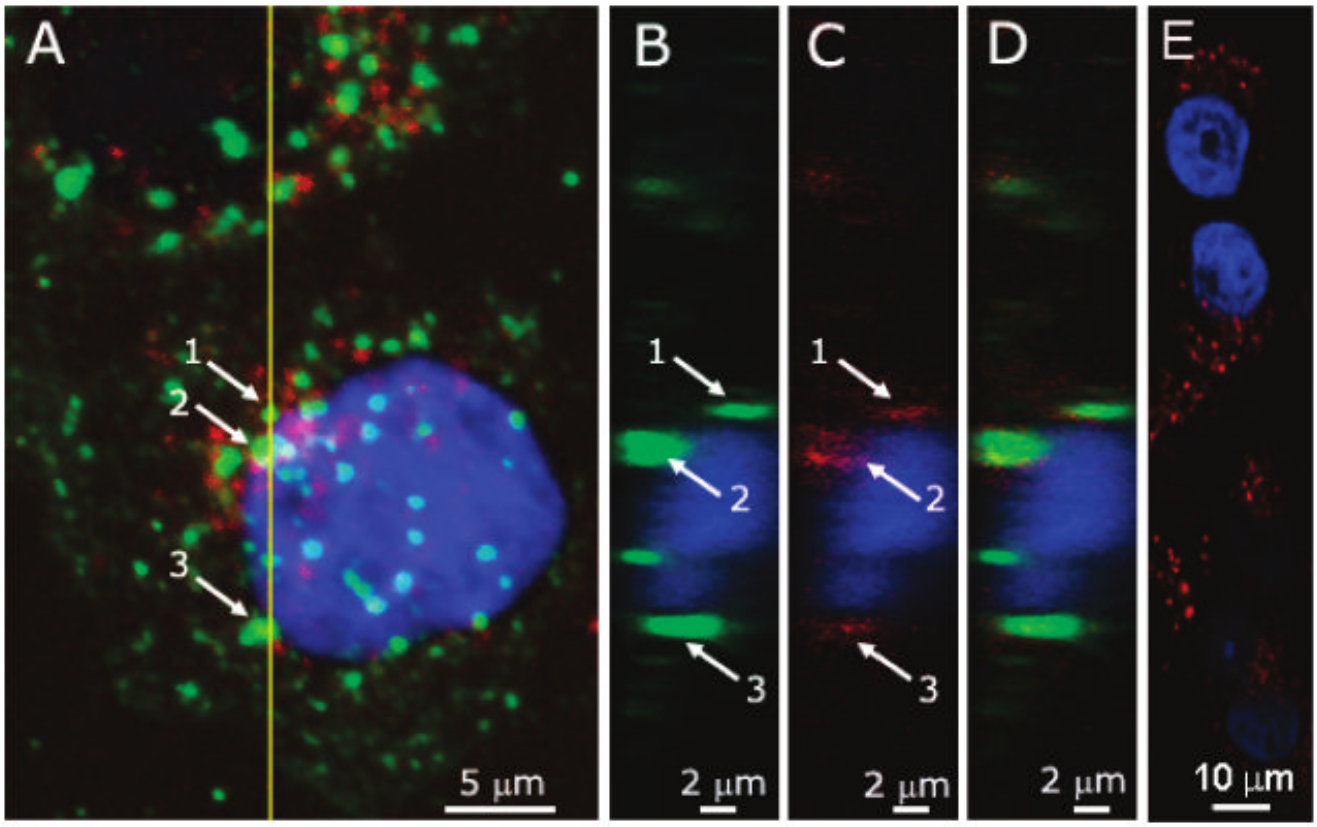

Figure 3.

Confocal microscopic analysis of the uptake of G5-NH_2-AF into the lysosomal compartments. KB cells grown on coverslips were incubated with 3 μM G5-NH_2-AF (green) and LysoTracker Red (red) for 1 h, fixed with paraformaldehyde, mounted using solution containing the nuclei stain DAPI (blue), and the fluorescence was measured as given in the Experimental Section. The Maximum Projection Image, shown in A, is obtained through individual *z*-series images. B, C, and D were obtained from the image shown in A, taken through the *y*–*z* slice along the indicated yellow line. A and D show all three of the stains, B shows the G5-NH_2-AF and nuclei stains, and C shows the LysoTracker Red and nuclei stains. The composite image of the blue, green, and red stains of control cells treated with PBS in place of the dendrimer is shown in E, imaged under identical conditions. The arrows represent three different lysosome-containing regions, depicting the colocalization of green and red fluorescence.

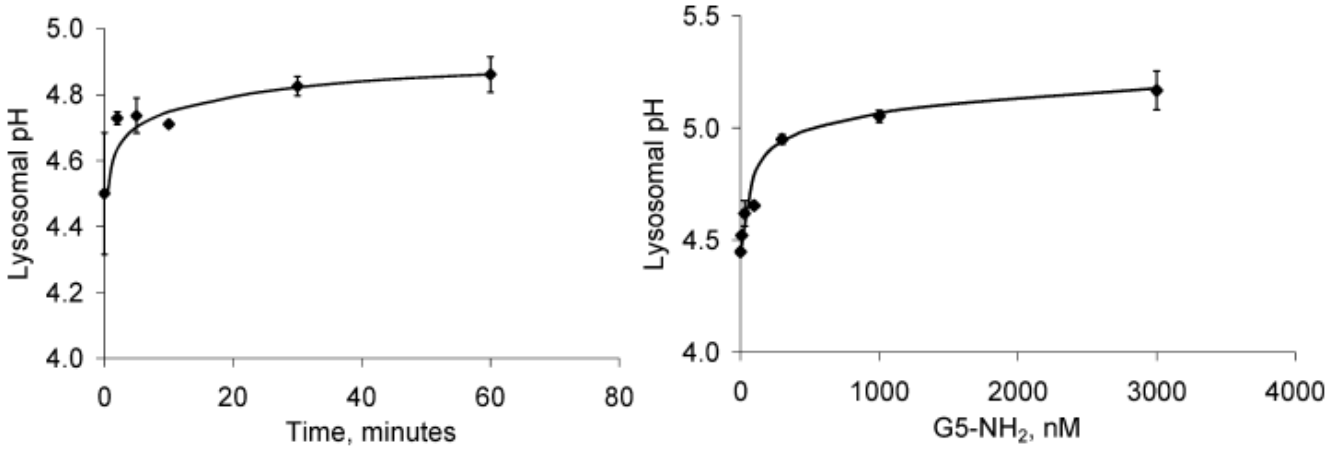

Figure 4.

Effect of primary amine-terminated PAMAM dendrimer on lysosomal pH. Left: KB cells were incubated with 300 nM amine-surfaced G5-PAMAM dendrimer for different time periods at 37 °C, and the lysosomal pH was determined as given in the Experimental Section. Right: Dose response under similar conditions, incubated with the dendrimer for 1 h.

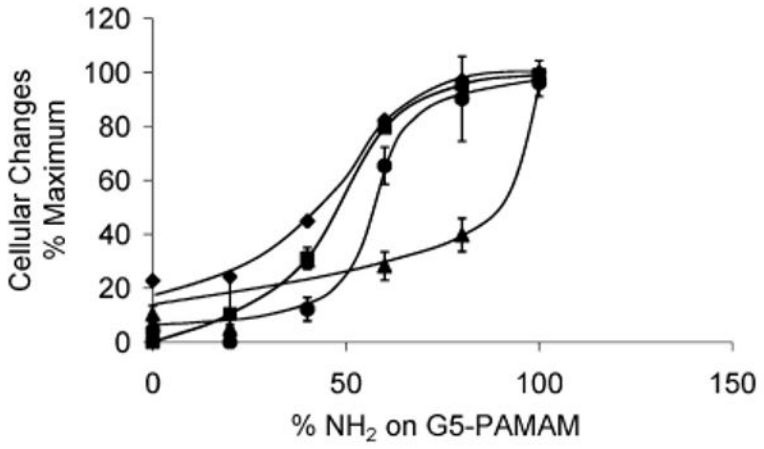

Figure 5.

Effect of increasing the number of PAMAM primary amine groups on cytotoxicity and lysosomal pH. KB cells were incubated at 37 °C with 3 μM each of the PAMAM dendrimer containing different percentages of surface primary amine groups, and the acute cytotoxicity was determined by flow cytometry from the percent dead cells identified in the forward scatter/side scatter plots (diamond symbols, 1 h incubation) and by LDH release (triangle symbols, 2 h incubation). The changes in lysosomal pH were measured in Dextran-FITC loaded cells following a 1 h incubation with the dendrimer (circle symbols). The effect of the compounds on the inhibition of cell proliferation was tested by XTT assay (square symbols, 3 days' incubation). The data represent the percent maximal changes obtained, giving 100% for the fully amine-surfaced dendrimer.

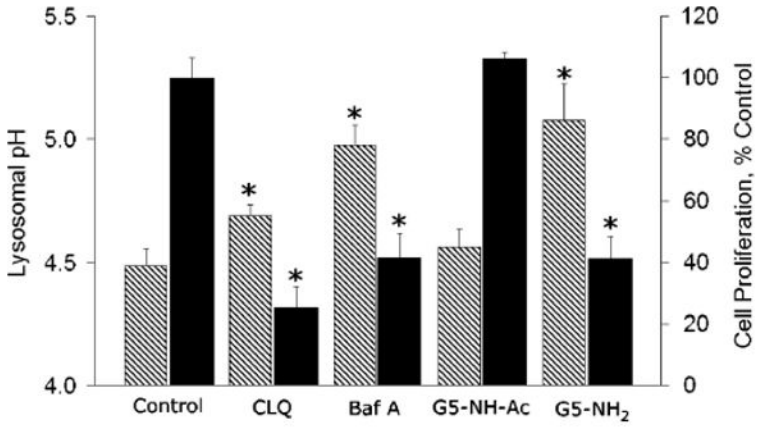

Figure 6.

Effects of lysosomotropic agents on cell growth and lysosomal pH. KB cells were incubated for 1 h (for lysosomal pH measurement) or 3 days (for XTT cell growth assay) with chloroquine (CLQ, 100 μM), bafilomycin A1 (Baf A, 500 nM), 100% acetylated PAMAM (G5-NH-Ac, 1 μM), or 100% amine-terminated PAMAM (G5-NH_2, 1 μM); the lysosomal pH (shaded bars) and XTT cell proliferation (solid bars) assays were performed as described in the Experimental Section. *$p < 0.05$ vs respective controls.

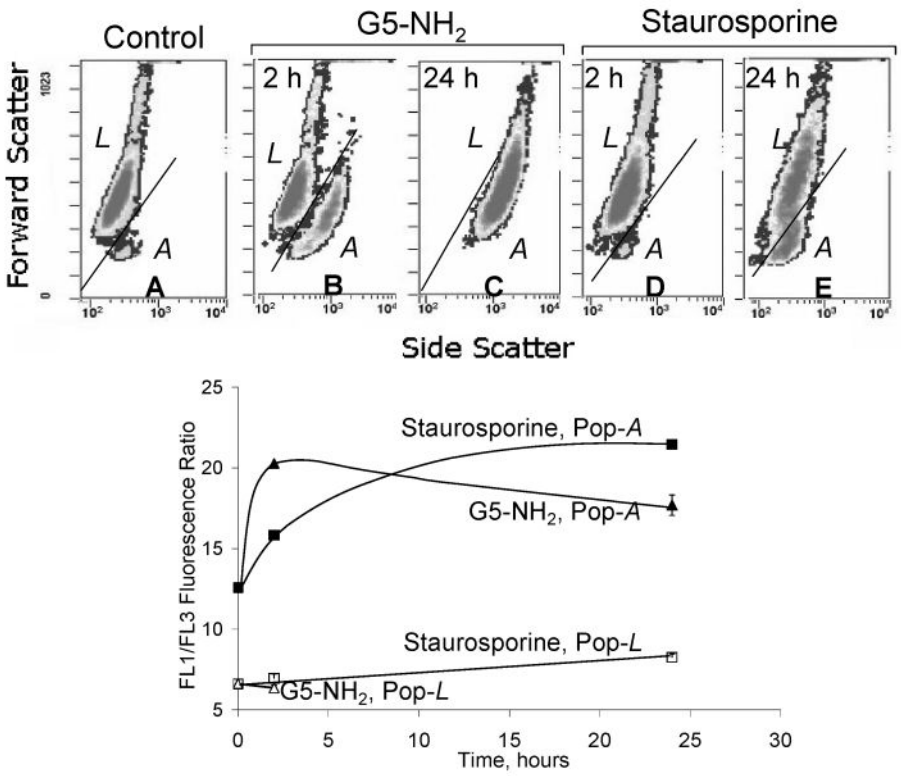

Figure 7.

Induction of mitochondrial transmembrane potential changes by 100% amine-terminated G5-NH_2. KB cells were incubated with G5-NH_2 or staurosporine, and the mitochondrial transmembrane potential was assessed by a MitoCapture, a flow cytometry-based mitochondrial apoptosis detection system described in the Experimental Section. Upper panel: Contour plots of forward scatter vs side scatter of control cells (A); cells treated with 3 μM G5-NH_2 for 2 and 24 h (B, C); and cells treated with 5 μM staurosporine for 2 and 24 h (D, E). *L* and *A* represent the live and apoptotic/dead cell populations, respectively. Lower panel: MitoCapture assay showing the time-dependent increases in the FL1/FL3 ratio of the two cell populations shown in the upper panel, indicative of apoptosis through the mitochondrial pathway.

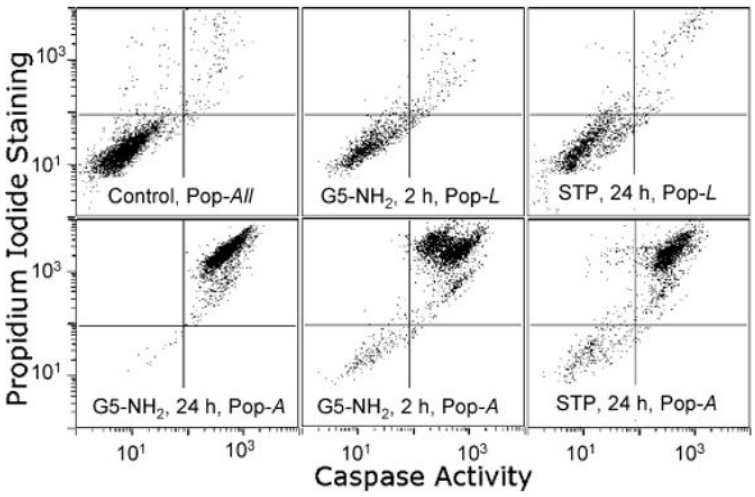

Figure 8.

Determination of caspase activity following treatment with 100% amine-terminated G5-NH_2. KB cells were incubated with G5-NH_2 (3 μM) or staurosporine (STP, 5 μM) for the indicated time periods shown, and the caspase activity was quantified using flow cytometry by the CaspaTag detection system, as described in the Experimental Section. The data shown are for the two populations of cells (Pop-*L* and Pop-*A*) identified by the forward scatter/side scatter plots as shown in Figure 7 (upper panel). The assay is based on the fluorescence emission of a cell-permeable caspase inhibitor that binds only to activated caspases 3 and 7. As shown in Figure 7 (upper panel), 24 h treatment with G5-NH_2 resulted in all the cells to appear in the population *A*, and at 2 h, the staurosporine failed to show a significant increase in population *A* (not shown).